Field Crops Research 234 (2019) 95–106

Contents lists available at ScienceDirect

Field Crops Research

journal homepage: www.elsevier.com/locate/fcr

Estimating cropland carbon fluxes: A process-based model evaluation at a Swiss crop-rotation site

Andrew Revill[a,*], Carmen Emmel[a], Petra D'Odorico[a,b], Nina Buchmann[a], Lukas Hörtnagl[a], Werner Eugster[a]

[a] Department of Environmental Systems Science, Institute of Agricultural Sciences, ETH Zurich, 8092 Zurich, Switzerland
[b] Department of Biology, University of Toronto, Mississauga, ON L5L1C6, Canada

ARTICLE INFO

Keywords:
Cropland carbon budget
Crop carbon dioxide simulation
Crop growth simulation
Pea crop development

ABSTRACT

In support of climate change mitigation strategies and food security, there is an ever-increasing requirement to understand the key drivers of cropland yields and carbon (C) budgets. Process-based crop models, driven by meteorological observations, can provide realistic simulations and diagnosis of the variability in crop C budgets. However, the field-scale observations required to validate the models, particularly across multiple growing seasons and crop types, are seldom available.

This research evaluates the Soil-Plant-Atmosphere Crop (SPA-Crop) model for estimating the C fluxes of multiple crop types and seasons at the Swiss long-term flux site Oensingen (CH-OE2). SPA-Crop is a detailed parametric model, simulating ecosystem photosynthesis and water balance at fine temporal (half-hourly time-steps) and vertical scales (multiple canopy and soil layers). We initialised the model at the point-scale using management information and meteorological observations recorded during ten crop seasons from 2004 to 2015. SPA-Crop has been developed for simulating winter cereals (wheat and barley), we further evaluated the model performance for these crops at CH-OE2 and extended the simulation to include a crop-specific calibration for winter rapeseed and pea crops. Model estimates of net ecosystem exchange (NEE) of carbon dioxide (CO_2), ecosystem respiration (R_{eco}), and gross primary production (GPP) were evaluated based on gap-filled and partitioned eddy covariance (EC) fluxes. Further comparisons were made between modelled and observed yields.

The daily SPA-Crop estimates had a high agreement with the EC measurements across the different crop types with a mean R^2 of the NEE of 0.74 (wheat), 0.73 (barley), 0.71 (rapeseed) and 0.69 (pea). The modelled yield estimates had biases ranging from −22% (barley, measured-model difference −70 gC m^{-2}; 0.31 t ha^{-1}) to +56% (rapeseed, measured-model difference −85 gC m^{-2}; −0.38 t ha^{-1}), with the largest bias of wheat being only −13% (measured-model difference 34 gC m^{-2}; 0.15 t ha^{-1}) across four wheat seasons. We recommend future SPA-Crop developments – particularly with regards to improving the precision of R_{eco} estimates. Our research demonstrates that SPA-Crop is a reliable tool for simulating the C budget and yield across the four crop types: winter wheat, winter barley, winter rapeseed, and peas.

1. Introduction

Crop growth is strongly influenced by climate (Hansen, 2002). Croplands are also entirely managed ecosystems, with human intervention being applied on a range of spatial and temporal scales (Porter and Semenov, 2005; Reichstein et al., 2013). This management, including tillage and harvesting events, results in changes to soil and vegetation carbon (C) pools, thus generating significant land-atmosphere carbon dioxide (CO_2) fluxes (Ceschia et al., 2010; Smith et al., 2010). Therefore, understanding the impacts of climate change and adaptive management strategies on crop production, and the subsequent CO_2 fluxes, is essential for sustaining human life and environmental well-being (Zhang et al., 2007; Matthews et al., 2013). Process-based crop models are increasingly used as a tool for quantifying and investigating these climate and management effects on crop growth. In this study, we adapted the Soil-Plant-Atmosphere Crop model (SPA-Crop; Sus et al., 2010) to a typical 4-year crop rotation containing crop types, including rapeseed and peas, which were poorly represented by existing crop models.

Generally, intra-annual cropland C dynamics are characterised by

* Corresponding author at: School of Geosciences, University of Edinburgh, Crew Building, The King's Buildings, Edinburgh, EH9 3FF, United Kingdom.
E-mail address: a.revill@ed.ac.uk (A. Revill).

https://doi.org/10.1016/j.fcr.2019.02.006
Received 20 April 2018; Received in revised form 3 January 2019; Accepted 5 February 2019
Available online 23 February 2019
0378-4290/ © 2019 Elsevier B.V. All rights reserved.

an increasingly strong CO_2 uptake during vegetative growth that is then reduced during the reproductive phase, with the cropland becoming a net C source at or around senescence. However, these fluxes vary in response to climate, crop type, and the timings and type of management (Lehuger et al., 2010). Eddy covariance (EC) flux towers, including those available in the global FLUXNET network (Baldocchi et al., 2001), do provide continuous observations of cropland ecosystem net CO_2 fluxes (Moureaux et al., 2008; Eugster et al., 2010; Moureaux et al., 2012). EC measurements are available for multiple locations, climate regimes, crop types, and seasons. Nonetheless, at the global scale, these site-level observations are poorly distributed both temporally and spatially, thus causing fluxes related to crop growth and management to be grossly under-sampled (Zheng et al., 2014). Alternatively, process-based crop models (referred to henceforth as crop models) can simulate the key mechanisms that result in gains or losses of C within a cropland ecosystem, including the processes linked to photosynthesis and ecosystem respiration (Lehuger et al., 2010; Boote et al., 2013). Typical crop models targeting yield estimates are successful with daily (or longer) timesteps (e.g., Kollas et al., 2015). However, biogeochemical or soil-vegetation-atmosphere-transfer-scheme (SVAT) based crop models can provide a more comprehensive analysis of factors determining the cropland C budget. Since these models work with hourly timesteps, they allow for comparisons with direct observations of the net ecosystem exchange (NEE) of CO_2 measured at EC towers. The models can also be used as a synthetic tool for investigating the behaviour of cropland ecosystems under differing soil, vegetation, and meteorological conditions with management regimes (Challinor et al., 2014; Webber et al., 2014; Parkes et al., 2018). The information on cropping systems has contributed to research and policy-making related to climate change and food security (Matthews et al., 2013; Ewert et al., 2015). For instance, recent crop modelling research has investigated crop yield responses to realistic CO_2 emission scenarios (e.g., Angulo et al., 2013), heat stress (e.g., Deryng et al., 2011; Gabaldón-Leal et al., 2016), and for quantifying the impacts of direct and diffuse solar radiation (e.g., Mercado et al., 2009).

Some crop models primarily aim at annual yield estimates and thus are sufficiently accurate with daily and longer timesteps. Other crop models are often crop-specific and can resolve short-term leaf-level processes over multiple canopy layers. Therefore, these detailed models require and can thus be applied using high resolution (e.g., half-hourly) meteorological driving data, along with variables related to soil characteristics, plant traits, and management practices. In addition to these considerable input demands, when compared to standard land-surface models, crop models often consist of extensive parameterisations that can only be calibrated from field experiments (Therond et al., 2011; Valade et al., 2013). However, the necessary field-scale observations are temporally and spatially sparse. Thus the data required to apply these complex models are seldom available (Gabaldón-Leal et al., 2016).

In addition to the model input data, a scarceness of reliable yield and EC data further limits the extent to which crop models can be improved and evaluated – particularly for the simulation of multiple crop types and growing seasons. White et al. (2011) highlight that past crop modelling research has predominantly focused on the four most common crop types: wheat, maize, rice, and soybean. To our knowledge, no other modelling study has included peas and only a limited number of crop modelling studies, which include SPA-Crop, has demonstrated a capacity to simulate additional crop types, such as rapeseed (e.g., Huang et al., 2009) and barley (Rötter et al., 2012; Abi Saab et al., 2015). In this research, we use the measurements at the Oensingen Swiss FluxNet cropland site, which contributes to FLUXNET, to drive and evaluate SPA-Crop for the simulation of wheat, barley, rapeseed, and pea crops. Furthermore, few studies (e.g., Dietiker et al., 2010) have performed a model analysis of multiple crop growing seasons in a crop rotation system at a single site. Past crop modelling studies, including those at Oensingen (e.g., Hastings et al., 2010; Sus et al., 2010; Wattenbach et al., 2010; Revill et al., 2013; Vuichard et al., 2016) have often focused on one winter cereal crop cycle per site. Measurements at Oensingen – covering the soil, atmosphere, and vegetation domains at up to half-hourly resolutions – span a relatively long period (> 10 years) when compared to other arable research sites with flux data available on the FLUXNET network. Consequently, the uniqueness of our research is the use of these data-rich measurements in order to thoroughly evaluate SPA-Crop for simulating multiple crop types and seasons.

Our study objectives were to: (1) Quantify the performance of SPA-Crop for simulating the major fluxes and C stocks determining the cropland C budget: gross primary production (GPP), total ecosystem respiration (R_{eco}), NEE, and yield. This model evaluation is based on measured EC fluxes and the reported yield over ten crop growing seasons from 2004 to 2015, including that of winter wheat, winter barley, winter rapeseed, and peas. (2) Identify model deficiencies and, subsequently, provide recommendations for further SPA-Crop model developments.

2. Data and methods

2.1. Site description

We evaluated the performance of SPA-Crop for a total of ten crop growing seasons, between 2004 and 2015, at a 1.55 ha field located on the Central Swiss Plateau region near the town of Oensingen (Canton of Solothurn, Switzerland; 47°17'11.1" N, 7°44'01.5" E, 452 m a.s.l.). Throughout our study period, the Oensingen site had a mean temperature of 9.7 °C and an annual precipitation of around 1100 mm. The site soil was formed from alluvial deposits to a depth of 1.6 m. From Alaoui and Goetz (2008), the Oensingen soil can be described as silty clay to a depth of 0.8 m with a texture comprising of 42% clay, 33% silt and 25% sand. The organic matter content varied from 2.8% in the top soil to 0% in the subsoil.

Site management included rotating the crop types grown each year. For our analysis, we included four winter wheat (*Triticum aestivum* L.),

Table 1
Summary of crop types, seasons and manure applications (from 2004 to 2015) at the Oensingen site. Note: Although a potato season (2006) existed within this crop rotation period, due to severe hail damage, this crop was not harvested and, consequently, not included in this analysis.

Season	Crop type	Sow day	Harvest day	Manure application day	Manure type (amount; g C m^{-2})
1	Winter barley	29/09/2004	14/07/2005	–	–
2	Winter wheat	19/10/2006	15/07/2007	24/01/2006	Solid (147.71)
3	Rapeseed	28/07/2007	16/07/2008	–	–
4	Winter wheat	07/10/2008	21/07/2009	–	–
5	Peas	09/05/2010	19/07/2010	04/08/2009	Liquid (8.36)
6	Winter wheat	15/10/2010	02/08/2011	06/05/2010	Solid (114.51)
7	Winter barley	24/09/2011	09/07/2012	02/09/2011	Liquid (16.32)
8	Rapeseed	04/09/2012	28/07/2013	28/08/2012	Liquid (24.48)
9	Winter wheat	19/10/2013	24/07/2014	24/09/2013	Liquid (24.48)
10	Winter barley	29/09/2014	04/07/2015	12/09/2014	Liquid (24.48)

three winter barley (*Hordeum vulgare* L.), two winter rapeseed (*Brassica napus* L.) and one pea (*Pisum sativum* L.) growing season. Mineral fertilisers were applied during all of these crop seasons (see Table 1). Although, an additional pea crop season was included in the Oensingen crop rotation in 2016, during this growing period, the field site was largely water logged, leading to partial failure of crop establishment and was, thus, not considered in our analysis. In accordance with the Swiss integrated management framework of the Proof of Ecological Performance (The Swiss Federal Council, 2015), the site has a typical winter wheat dominated crop rotation, whereby winter wheat is grown approximately every second year with other crops grown in the intervening years.

2.2. Data acquisition and processing

2.2.1. Meteorological measurements

Meteorological data at half-hourly resolution, which were required to drive SPA-Crop, were available at Oensingen for each of the ten crop growing seasons. The specific meteorological variables used in this study included air temperature (°C), atmospheric CO_2 concentration (ppm), wind speed (m s^{-1}), short-wave radiation (W m^{-2}), relative humidity (%), photosynthetic photon flux density (μmol m^{-2} s^{-1}), precipitation (mm), and atmospheric pressure (hPa).

Pre-processing steps, consisting of screening and gap-filling, were applied to the meteorological variables to produce a reliable and continuous dataset covering the entire study period. The screening procedure entailed analysing the temporal variability of each variable, whereby abnormalities, due to instrumental or user error, were identified and subsequently removed. Instrument failure and maintenance combined with the removal of observations during screening, introduced additional gaps in the time-series of meteorological data. These gaps were filled according to a hierarchical procedure (see further details on the gap-filling in the online supplementary material section A).

2.2.2. NEE flux calculation and partitioning

NEE (i.e., NEE = GPP − R_{eco}) was measured at the Oensingen site with an open-path infrared gas analyser (LI-7500, LI-COR, Lincoln, NB, USA) and a three-dimensional sonic anemometer (R3-50, Gill Inst. Ltd, Lymington, UK), which were located in the centre of the field at a height of two metres throughout the study period. NEE was determined using the eddy covariance software EddyPro (version 6.2.0, LI-COR) following the approach outlined in Moureaux et al. (2012). The NEE data were despiked, according to Rogiers et al. (2005), and then quality-controlled, gap filled and partitioned into GPP and R_{eco} that were used as reference to evaluate the SPA-Crop outputs. Using the REddyProc R package (Max Planck Institute for Biochemistry; http://r-forge.r-project.org/projects/reddyproc), we applied the filtering and partitioning algorithm based on that of Reichstein et al. (2005) for deriving R_{eco} from night-time NEE data. NEE data were filtered to remove observations made under low-turbulence conditions based on a u_*-threshold criteria. The applied despiking and u_* filtering procedures reduced the measured NEE data by an average of 45% per year; ranging between 27% (2006 to 2007) and 51% (2004 to 2005 and 2012 to 2013). The partitioning was then applied to the filtered datasets whereby R_{eco} was separated from the remaining night-time NEE observations using the short-term temperature sensitivity parameter, E_0, which was estimated using an exponential regression model (Eq. (1), Lloyd and Taylor, 1994):

$$R_{eco} = R_{ref}\, e^{E_0(1/(T_{ref}-T_0)-1/(T-T_0))} \quad (1)$$

where the reference temperature parameter, T_{ref}, and regression parameter, T_0, were fixed at 10 °C and -46.02 °C, respectively, as in Lloyd and Taylor (1994). The temperature independent reference respiration, R_{ref}, was derived using nonlinear regression over consecutive 4-day periods by fixing all parameters in Eq. (1) except R_{ref}. Once the R_{ref} parameter was estimated for each period, linear interpolation was then applied to generate temporal values between these estimates; thus, allowing for the estimation of R_{eco}. Gap filling was then applied to the filtered NEE dataset using the Marginal Distribution Sampling method (Reichstein et al., 2005).

2.3. SPA-Crop model

2.3.1. Model description

SPA-Crop (available at: https://sourced.ecdf.ed.ac.uk/projects/geos/SPA) simulates the ecosystem C cycle and water exchanges at fine temporal scales (half-hourly time-steps) and vertical resolutions (up to ten canopy layers). This simulation includes the integration of multiple leaflevel processes, including photosynthesis using the Farquhar model (Farquhar and von Caemmerer, 1982) and evapotranspiration using the PenmanMonteith equation (Jones, 2013). These processes, which are scaled up to make canopylevel predictions, are linked to a radiative transfer scheme – tracking absorption, reflectance, and transmittance of direct and diffuse irradiance. As detailed in Williams et al. (2001), this canopy radiative transfer scheme also determines the soil surface temperature – a balance of net radiation from down-welling radiation and long-wave losses from the soil surface with sensible, latent, and ground heat fluxes.

The model links photosynthesis and transpiration estimates at leaflevel by a model of stomatal conductance, which is similar to the mechanism proposed by Cowan (1978). Specifically, the stomatal conductance adjusts accordingly to balance transpiration with the rate of water supply. The maximum water supply rate is determined by the minimum leaf water potential, canopy capacitance, root water uptake, soil water availability and stem hydraulic conductance (Williams et al., 1996, 2001). To prevent xylem cavitation, the stomatal closure can occur at a minimum leaf water potential. Once the minimum leaf water potential has been reached, the sustainable water flux rate includes a dependency on the hydraulic resistance. The soil and root components of hydraulic resistance calculated at the soil layers are summarised in section B of the online supplementary information.

To provide a realistic simulation of crop growth and biomass accumulation, SPA-Crop uses crop-specific look-up tables that define the fraction of assimilated CO_2 that is partitioned amongst the roots, leaves, stem and storage organs (i.e. grain, rapeseeds or peas) as a function of development stage. The development stage is calculated as the accumulation of daily development rates – a function of temperature, photoperiod and vernalisation (until emergence, Streck et al., 2003). We acknowledge that water stress can have an influence on crop development (Penning de Vries et al., 1989; Begcy and Walia, 2015), however, from the Oensingen site management there were no reports of significant drought periods.

The R_{eco} is calculated as the sum of the SPA-Crop estimates of crop autotrophic and soil heterotrophic respiration. The model simulates autotrophic respiration as a fixed fraction of GPP, which varies amongst the different crops (Table 2). The components of heterotrophic respiration, modelled independently of crop type, include the mineralisation of the surface litter and soil organic C (SOC) pools. The C in the surface litter pool is also allocated to the SOC pool via a decomposition flux, which is determined by the size of the litter pool and the decomposition rate. The litter and SOC pool respiration are calculated as a function of the litter and SOC content, a specific C mineralisation rate (set differently for the two components) and temperature (based on a Q_{10} temperature relationship).

SPA-Crop divides the soil into layers of constant thickness, where the soil temperature is modelled by determining the distribution of heat across these layers. This flux is based on the heat at the ground (determined using the SPA-Crop canopy radiative transfer scheme), the thermal gradient between soil layers and the soil thermal conductivity (Williams et al., 2001). These thermal parameters are further dependent on the SOC, soil mineral content (i.e. fraction of clay and sand) and

Table 2
Summary table describing the crop-specific SPA-Crop model vegetation parameters that determine the structural, biochemical and optical properties of a crop canopy. Note: Only the model parameters that vary between the different crop types have been included here, a more comprehensive list of SPA-Crop parameters can be seen in Sus et al. (2010). The specific parameter values set for each crop type are included in Appendix section A.

Parameter type	Parameter description	Unit
Structural	Canopy layer heights	m
	Leaf area distribution	Fraction
	Leaf width	m
	Leaf angle distribution	Coefficient
	Maximum depth	m
	Critical leaf area	$m^2 m^{-2}$
Biochemical	Leaf water potential	MPa
	Fraction of GPP respired	%
	Maximum carboxylation capacity	$\mu mol\ m^{-2}\ s^{-1}$
	Maximum electron transport	$\mu mol\ m^{-2}\ s^{-1}$
	Leaf carbon per area	$gC\ m^{-2}$
	Leaf nitrogen per area	$gN\ m^{-2}$
	Leaf nitrogen distribution	Fraction
Phenology	Development pre-anthesis	Coefficient
	Development post-anthesis	Coefficient
	Temperature sum at emergence	Degree days
	Minimum temperature for development	°C
	Optimum temperature for development	°C
	Maximum temperature for development	°C
	Minimum temperature for vernalisation	°C
	Optimum temperature for vernalisation	°C
	Maximum temperature for vernalisation	°C
Optical	Critical photoperiod	Hours
	Photoperiod sensitivity	Coefficient
	Leaf NIR reflectance	%
	Leaf NIR transmittance	%
	Leaf PAR reflectance	%
	Leaf PAR transmittance	%

soil water content (Hillel, 1980). The modelled changes in soil water content are also used to calculate the redistribution of thermal energy throughout the soil layers. Specifically, the change in heat at a given soil layer is calculated based on the change in soil water content, current soil temperature and the heat capacity of water.

Changes to the modelled water content of each soil layer are controlled by precipitation and evaporation (at the surface layer), root water uptake and gravitational drainage. The water transport across each of the soil layers is modelled based on the Richards (1931) equations. Specifically, SPA-Crop uses the hydraulic functions and coefficients derived from Rawls et al. (1982), as summarised in Saxton et al. (1986), for deriving the soil-water potential and conductivity of each layer based on empirical relationships between soil texture (i.e. percentage of clay and sand) and moisture content. Surface runoff can also occur when the water content of the upper layer exceeds the calculated hydraulic conductivity.

2.3.2. Model parameterisation and calibration

SPA-Crop has previously been parameterised by Sus et al. (2010) over multiple European FLUXNET sites (including Oensingen) for the simulation of winter wheat and barley. In this study, we updated these parameter values based on field-scale measurements collected during several consecutive field seasons, between 2004 and 2015, and included new parameter values in order to model winter rapeseed and pea crops. These crop-specific parameters included those that were related to the vegetation and C allocation. Primarily, these parameter values were updated based on field measurements, however if unavailable, values were either used from literature or, as was the case for pea crops, were inferred via model calibration (see table in the online supplementary information).

The model calibration procedure first involved defining the realistic limits of each of the missing parameter values based on the field observations and from literature for similar crop types. With the minimum and maximum values set for each of the missing parameters, we then performed a large ensemble of SPA-Crop model runs (4000). Each model run involved randomly sampling a value within the minimum/maximum parameter space and the resultant NEE flux estimates were compared to the corresponding EC data. We selected the set of model parameters that provided the highest agreement to the EC data.

For each crop type, the crop vegetation parameters can generally be categorised as the values that determine the structural, biochemical, phenological and optical properties of the crops (Table 2; see also online supplementary information). The vegetation structural and biochemical parameters also included defining the vertical distribution of total leaf area and nitrogen content across the simulated canopy layers. In this analysis, the number of crop canopy layers simulated by SPA-Crop, which we selected according to crop height (i.e. more layers were included for taller crops), were set at seven (winter wheat and barley), eight (winter rapeseed), and six (pea).

The SPA-Crop soil parameters included the initial C values for the surface litter (i.e. from crop residue) and soil organic C (SOC) pools and the corresponding decomposition rates, for the simulation of heterotrophic respiration. The litter C contents were derived from samples collected on 14th July 2005 (i.e. the day of the 2004/2005 winter barley harvest), which was determined as 190 $gC\ m^{-2}$. For subsequent simulated seasons, when detailed in the Oensingen management history, we estimated C litter content based on the recorded fraction of crop biomass remaining in the field after harvest. Further to the crop residue, the C litter pool also included manure that was reported to have been applied to the field prior to the sowing of selected crop seasons (Table 1). The soil C mineralisation rate parameters were set to 0.008 and $2.28 \times 10^{-6}\ hr^{-1}$ for litter and SOC, respectively (inferred from Buyanovsky and Wagner, 1987).

SOC content was defined as the amount of C per unit surface area in the soil layer 0.0–0.3 m which corresponds with the ploughing depth at Oensingen and other typical conventional tillage systems (Abdalla et al., 2013). Estimates of SOC were 7073 $gC\ m^{-2}$ (0–0.3 m topsoil layer) based on sampling conducted on 23rd August 2005 (as detailed in Alaoui and Goetz, 2008). The model's percentages of clay and sand within each soil layer were fixed at 42% and 25% based on measurements detailed in Alaoui and Goetz (2008), respectively. In addition to the litter and SOC, SPA-Crop also requires estimates of the seed C content, which represents the initial C source available for growth. The seed C content estimates were based on the mean seed C content across a sample size (> 30 seeds) for each crop type.

For the C allocation to the crop organs, which is determined by the developmental stage, SPA-Crop was initialised with the C partitioning look-up table for each crop type. For winter wheat, winter barley and winter rapeseed, this C allocation information was available from empirical observations of crop growth cycles detailed in Penning de Vries et al. (1989). Since literature on pea crop allocations was unavailable, C analysis was carried out during the 2016 pea crop growing season at Oensingen. This analysis involved estimating the fraction of C contained in the root, stem, foliage and storage (i.e. pod) organs from pea crop samples collected on four different dates (see plots in the online supplementary information).

2.4. Model evaluation approaches

The parameterised and initialised SPA-Crop model was run individually for each of the crop seasons using the gap-filled meteorological data. We evaluated the SPA-Crop simulation of the daily, and at-harvest cumulative sum, of GPP, R_{eco}, and NEE fluxes, between sowing and harvest, based on the EC half-hourly gap-filled data. However, since NEE is calculated directly from EC measurements, as opposed to being derived through a partitioning model (i.e. in the case of GPP and R_{eco}), we consider a comparison to gap-filled NEE a more

reliable means of evaluating model performance.

Metrics used in the model evaluation include the coefficient of determination (R^2) between model data and measurements, root-mean-square-error (RMSE), normalised-mean-bias-factor (NMBF) and percentage relative error (Δ). The RMSE describes the average discrepancies between SPA-Crop and the EC data (Eq. (2)):

$$RMSE = \sqrt{\frac{\sum_{i=1}^{n}(M_i - O_i)^2}{n}} \quad (2)$$

where M_i and O_i represent the SPA-Crop and EC-derived values, respectively. $\bar{O}$ is the mean of the EC data, and n is the number of SPA-Crop and EC data (i.e. days). The NMBF provides a normalised indication of the extent to which SPA-Crop over- or underestimates the fluxes relative to the EC data. In comparison to alternative metrics, Yu et al. (2006) demonstrated that the NMBF provides a statistically robust measure of model bias – avoiding over-inflation due to low values in the reference dataset, whilst maintaining evaluation symmetry. Specifically, when the mean SPA-Crop value overestimates the EC data ($\bar{M} \geq \bar{O}$), the NMBF is (Eq. (3)):

$$NMBF = \sum \left[\frac{O_i}{\sum O_i} \frac{(M_i - O_i)}{O_i} \right] \quad (3)$$

For $\bar{M} < \bar{O}$ (i.e. underestimation, Eq. (4)):

$$NMBF = \sum \left[\frac{M_i}{\sum M_i} \frac{(M_i - O_i)}{M_i} \right] \quad (4)$$

If the NMBF is positive ($0 \leq 1$), then SPA-Crop overestimates the EC data, whereas negative values ($-1 \geq 0$) indicate that SPA-Crop underestimates the data (Yu et al., 2006). The Δ of NEE, GPP and R_{eco} are always expressed with respect to the EC data (Eq. (5)) and then converted to a percentage.

$$\Delta = \sum \frac{(M_i - O_i)}{O_i} \quad (5)$$

We summarised the overall precision of SPA-Crop for the simulation of cumulative gap-filled daily fluxes for each crop type when averaged across the growing seasons using a statistically normalised version of a Taylor diagram (Taylor, 2001; Kärnä and Baptista, 2016). A Taylor diagram is a graphical means of evaluating multiple aspects of model performance. For each flux, the diagrams represented the model's performance by a single point within a polar coordinate system, whereby R^2 is plotted on the polar angle and the normalised standard deviation (NSTD) is shown on the polar axis. The NSTD is used to indicate how closely the model estimates match the amplitude of the variations in the EC data. We therefore calculate NSTD by dividing the mean SPA-Crop standard deviation for each flux estimate by those of the corresponding EC reference data. Thus, for a given crop type, the closer the point is to 1 along the R^2 and NSTD axes then the greater is the agreement between the model and the EC-derived data.

3. Results

3.1. Daily flux evaluation

3.1.1. Winter wheat

Across the four wheat seasons, the model captured the seasonal trends in GPP (mean $R^2 = 0.82$; mean RMSE = 2.0 gC m^{-2} d^{-1}) (Fig. 1). Particularly the timings of vegetative and reproductive growth phases. However, some discrepancies between the magnitudes of GPP estimates existed around the time of peak productivity, whereby SPA-Crop underestimated the maximum GPP by an average of 5.2 gC m^{-2} d^{-1} (26%). Overall, the SPA-Crop GPP had a negative bias when compared to the EC estimates.

A high agreement existed between R_{eco} and the EC data (mean $R^2 = 0.69$; mean RMSE = 1.4 gC m^{-2} d^{-1}). However, there was a large discrepancy in R_{eco} at the beginning of 2006/2007 wheat growing season, when the EC-derived R_{eco} was 3.2 gC m^{-2} d^{-1} (20%) greater than that of the SPA-Crop estimates around the date of sowing.

There was a generally high agreement between the daily SPA-Crop and the EC measured NEE (mean $R^2 = 0.69$; mean RMSE = 1.3 gC m^{-2} d^{-1}) for each of the winter wheat crop growing seasons. However, there were some notable differences between the model and measurements, typically between May and July when the SPA-Crop maximum NEE (i.e. maximum C uptake) under-estimated EC measurements by up to 6.2 gC m^{-2} d^{-1} (46%) for the 2006/2007 wheat growing season.

3.1.2. Winter barley

The winter barley SPA-Crop GPP estimates had a high agreement to EC data (mean $R^2 = 0.82$; mean RMSE = 2.2 gC m^{-2} d^{-1}) (Fig. 2). Across the three barley growing seasons, SPA-Crop captured both the seasonality and the overall magnitudes of GPP well, with the mean difference in maximum productivity being only −3.1 gC m^{-2} d^{-1} (−15%). Overall, the model had only a slightly positive bias when compared to the EC data (mean NMBF = 0.05). Furthermore, the correlation between SPA-Crop and the EC data was relatively consistent for these growth periods, the R^2 ranged from 0.76 to 0.87.

A high agreement with EC data was also found for R_{eco} (mean $R^2 = 0.76$; mean RMSE = 1.3 gC m^{-2} d^{-1}). For all seasons, the maximum R_{eco} of winter barley was underestimated by SPA-Crop, with an overall mean difference of −2.4 gC m^{-2} d^{-1} (−14%).The SPA-Crop estimates of winter barley NEE also had a high agreement (mean $R^2 = 0.72$; mean RMSE = 1.6 gC m^{-2} d^{-1}) with the EC measurements. Furthermore, when compared to that of winter wheat, the maximum modelled NEE more closely matched the EC measurements – particularly for the 2011/2012 season where the difference in maximum NEE was only 0.65 gC m^{-2} d^{-1} (5%). The 2014/2015 season had the largest disparity when the magnitude of peak NEE was underestimated by 4.8 gC m^{-2} d^{-1} (32%).

3.1.3. Winter rapeseed

The winter rapeseed SPA-Crop GPP estimates had a high agreement with the EC data (mean $R^2 = 0.83$; mean RMSE = 1.6 gC m^{-2} d^{-1}) (Fig. 3). However, the simulated GPP for the two seasons significantly underestimated the peak productivity; the maximum GPP was underestimated by 8.3 gC m^{-2} d^{-1} (35%) and 5.3 gC m^{-2} d^{-1} (9%) for the 2007/2008 and 2012/2013 seasons, respectively, when compared to the EC data.

The SPA-Crop estimates of winter rapeseed R_{eco} were comparable to those of wheat and barley (mean $R^2 = 0.73$; mean RMSE = 1.0 gC m^{-2} d^{-1}).The SPA-Crop daily NEE estimates for winter rapeseed had a similarly high agreement with the EC fluxes to those of wheat and barley (mean $R^2 = 0.71$; mean RMSE = 1.1 gC m^{-2} d^{-1}). The peak NEE value (i.e. maximum uptake) was underestimated by the model by up to 3.2 gC m^{-2} d^{-1} (37%) for the 2012/2013 season.

3.1.4. Pea

The SPA-Crop GPP estimates had a high agreement to the EC-derived GPP ($R^2 = 0.83$; RMSE = 1.4 gC m^{-2} d^{-1}; Fig. 4) for the single pea growing season (2010). Generally, the model closely captured the timing of vegetative and reproductive periods of peas. Although the simulated maximum GPP under-estimated that of the EC data by 2.2 gC m^{-2} d^{-1} (15%), SPA-Crop had an overall small positive bias (NMBF = 0.01).

A weak agreement existed between the SPA-Crop R_{eco} estimates and the EC data ($R^2 = 0.61$; RMSE = 1.0 gC m^{-2} d^{-1}) for pea crops, with the model estimates having an overall negative bias (NMBF = −0.25). A similarly weak agreement existed between the simulated daily NEE and the EC fluxes ($R^2 = 0.58$; RMSE = 0.9 gC m^{-2} d^{-1}). The modelled NEE generally matched the timings of the EC fluxes, however, SPA-Crop underestimated the peak NEE by 3.5 gC m^{-2} d^{-1} (43%).

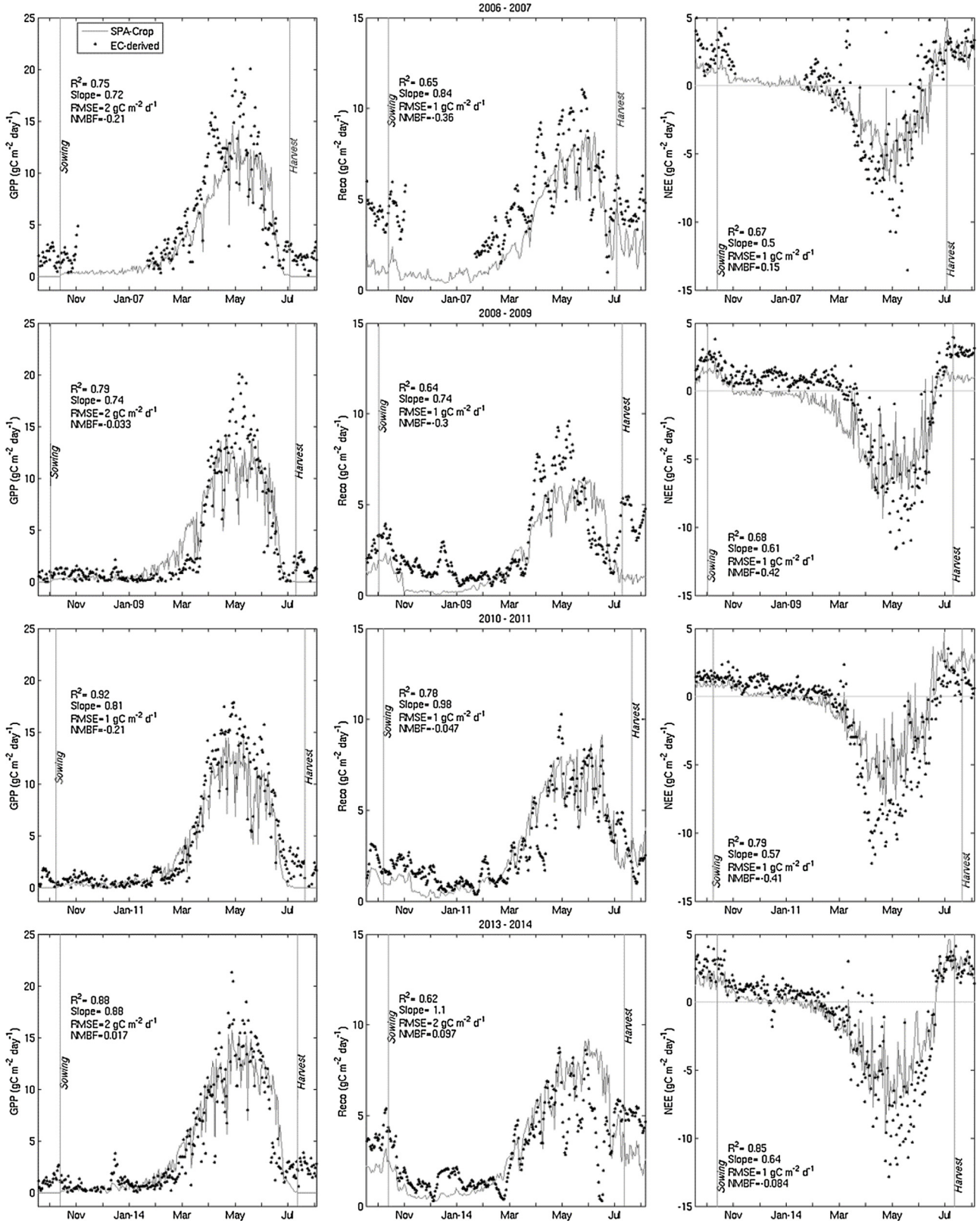

Fig. 1. Time-series plots comparing the SPA-Crop model and EC-derived estimates of GPP (left column), R_{eco} (middle column) and NEE (right column) between sowing and harvest for four winter wheat growing seasons at Oensingen (2006–2007, 2008–2009, 2010–2011 and 2013–2014). Metrics include the coefficient of determination (R^2) and the root-mean-square-error (RMSE).

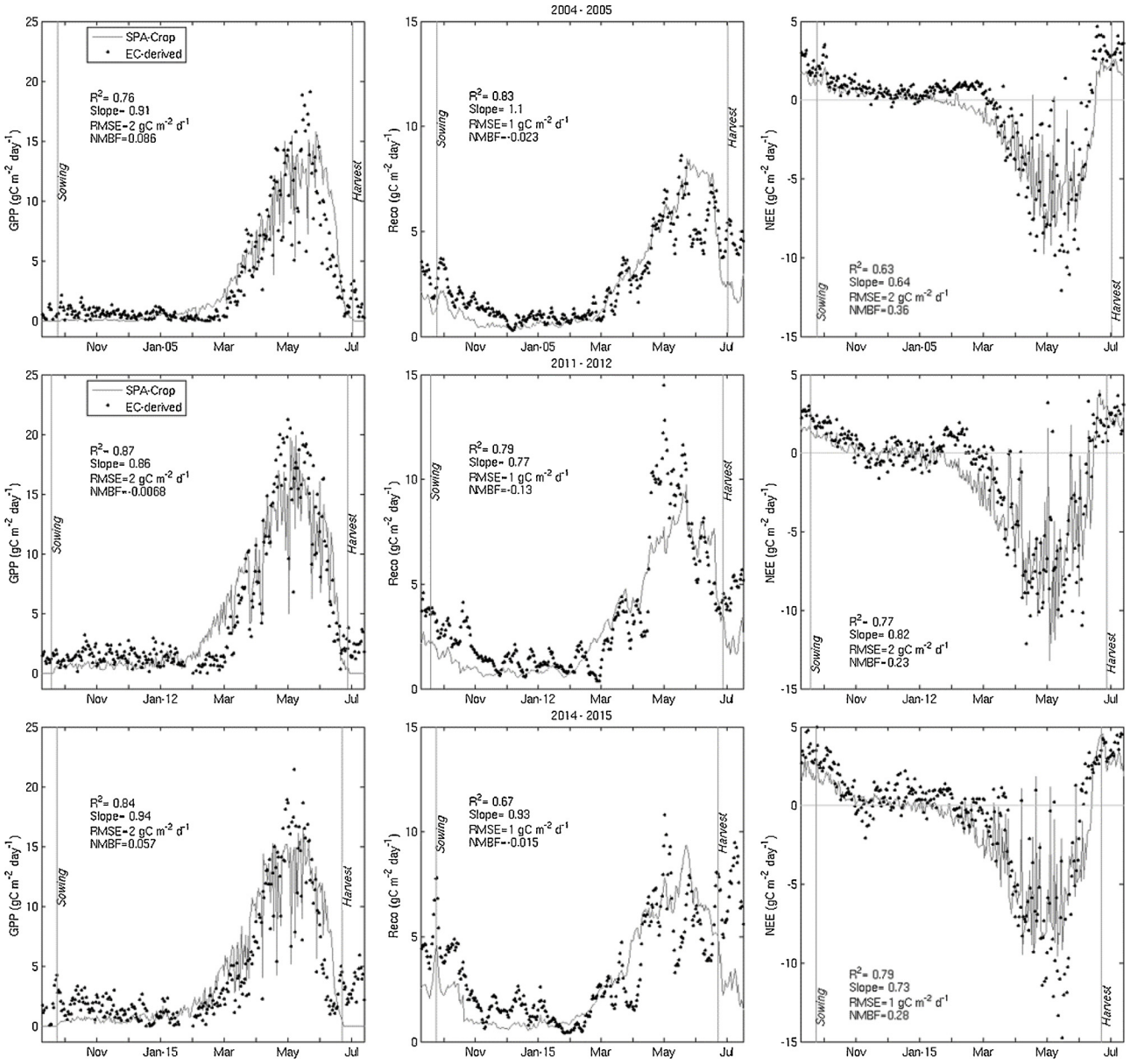

Fig. 2. Time-series plots comparing SPA-Crop model and EC-derived estimates of GPP (left column), R_{eco} (middle column) and NEE (right column) between sowing and harvest for three winter barley growing seasons at Oensingen (2004–2005, 2011–2012 and 2014–2015). Metrics include the coefficient of determination (R^2) and the root-mean-square-error (RMSE).

3.2. Crop season evaluations

3.2.1. At-harvest budgets and yield

From comparing the seasonal (i.e. sowing to harvest) sum of SPA-Crop flux estimates to those of the EC data (Table 3), for the majority of seasons the model overestimated the NEE flux sink strength. This NEE overestimation was most notable for the 2007 to 2008 rapeseed crop season, which had a Δ of +64% (Δ being the relative deviations from the mean). However, the cumulative SPA-Crop R_{eco} generally underestimated those of the EC data (Δ = −6%). The cumulative GPP differences were negative for both the rapeseed seasons (Δ = −11%) when compared to a relatively large positive difference in estimates for barley (Δ = +14%).

When comparing the SPA-Crop yield estimates to that recorded in the Oensingen site management across the ten seasons (Table 4), the model underestimates the observed yields for the majority of seasons. The modelled wheat yield estimates had the least bias with Δ ranging from −13% to +3%. However, SPA-Crop consistently underestimated the barley yield across the three seasons – Δ ranged from −22% to −16%. The rapeseed yield estimates had the largest inter-season range in model-observed differences; the Δ was −5% and +56% for the 2007 to 2008 and 2012 to 2013 seasons, respectively.

3.2.2. Crop type evaluation

From summarising the SPA-Crop performance on a per crop basis for the different fluxes (Fig. 5), all crop types exhibited a reasonable-to-high correlation with the EC-derived flux data ($0.59 \leq R^2 \leq 0.84$). The modelled estimates also matched the amplitude of the variations in the EC data, the NSTD was generally within ± 0.25. However, an exception to this similarity between model and EC data variability was for the winter wheat and pea crop NEE estimates, which had an NSTD of 0.71 and 0.68, respectively. The NEE estimates for winter barley had the highest agreement with the EC fluxes as all the R^2 values were greater than 0.73, and the NSTD was within ± 0.15 of the reference data.

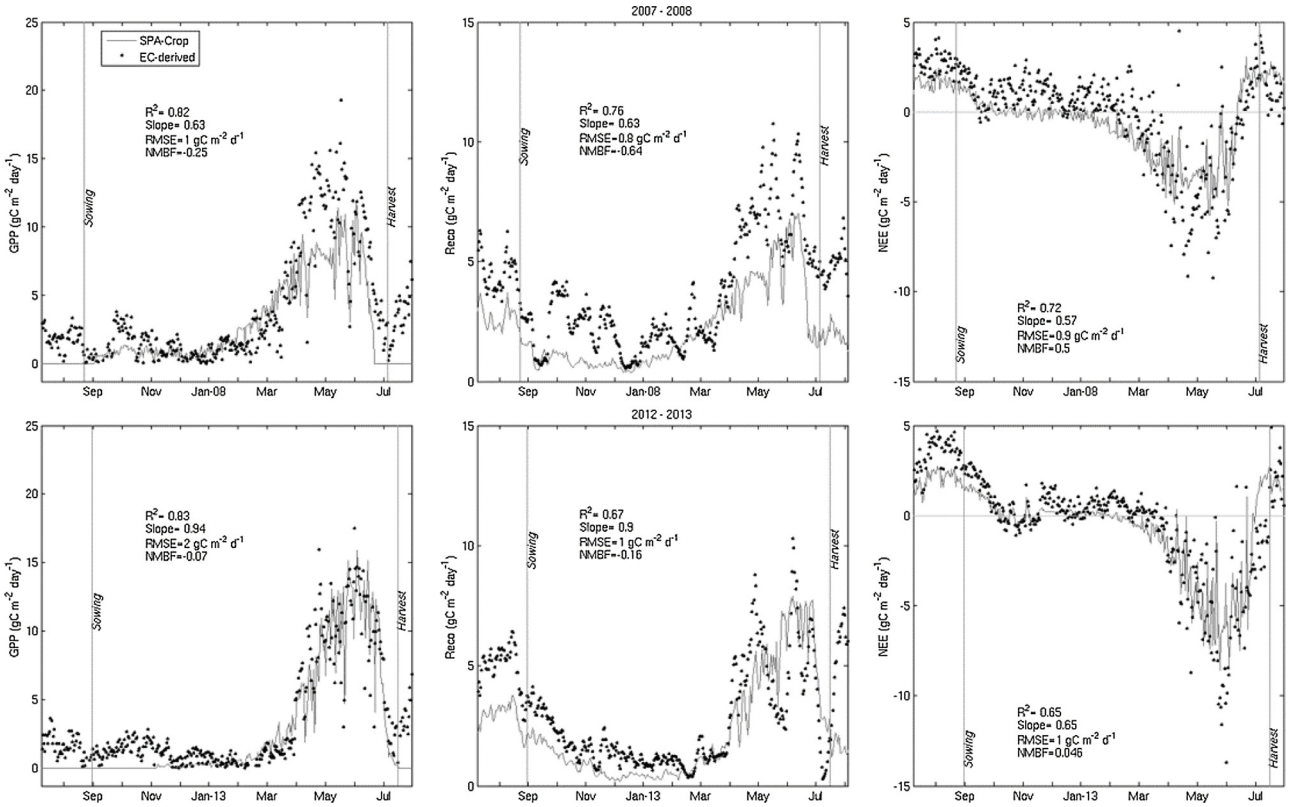

Fig. 3. Time-series plots comparing SPA-Crop model and EC-derived estimates of GPP (left column), R_{eco} (middle column) and NEE (right column) between sowing and harvest for two rapeseed growing seasons at Oensingen (2007–2008 and 2012–2013). Metrics include the coefficient of determination (R^2) and the root-mean-square-error (RMSE).

4. Discussion

4.1. SPA-Crop for daily carbon fluxes

The thorough evaluation and subsequent development of crop models are often challenged by a lack of measurements made at the field-scale (Gabaldón-Leal et al., 2016). Using detailed, high temporal resolution and long-term observations made at the Oensingen site, this study aimed to test the SPA-Crop model for simulating the key fluxes involved in the cropland C cycle. For all growing seasons, SPA-Crop was capable of capturing the seasonality of NEE fluxes with a high precision (mean R^2 = 0.72). Thus, although bias existed, the model generally captured the dynamics of the vegetative and reproductive growth stages of the four crop types included in this analysis.

The SPA-Crop was originally developed by Sus et al. (2010) for the simulation of winter cereal crops. Although we calibrated the model parameters for rapeseed and pea crops, these crop types are structurally contrasting to that of wheat and barley. The availability of the parameters values for winter rapeseed and pea crops from literature are also scarce when compared to that for wheat and barley. Consequently, it would have been anticipated that the model performance for these winter cereals would have been superior to that of rapeseed and pea. The modelled NEE estimates for the wheat and barley seasons closely matched the EC measurements (mean R^2 = 0.70; mean RMSE = 1.4 gC m^{-2} d^{-1}). However, a similarly high agreement was also achieved for the rapeseed and pea seasons (mean R^2 = 0.70; mean RMSE = 1.0 gC m^{-2} d^{-1}). Thus, the quality of the modelled GPP estimates was consistent for all crop types.

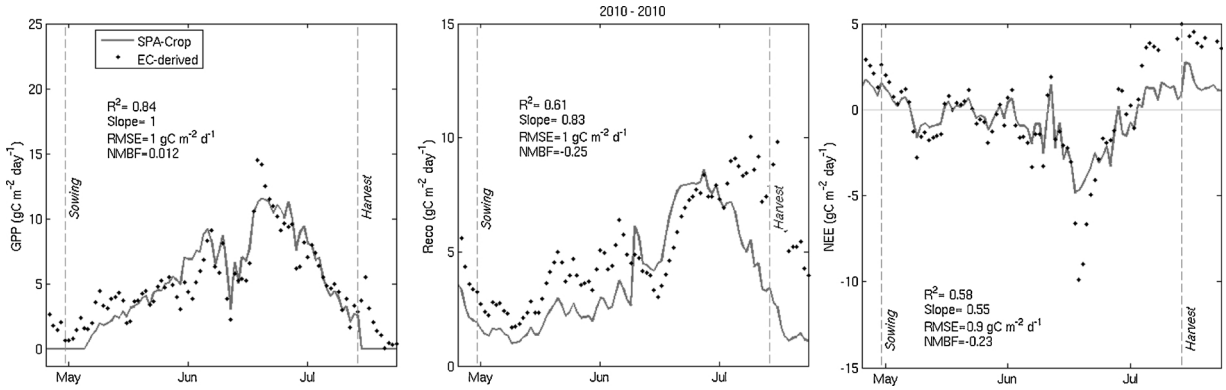

Fig. 4. Time-series plots comparing SPA-Crop model and EC-derived estimates of GPP (left column), R_{eco} (middle column) and NEE (right column) between sowing and harvest for a pea crop growing season at Oensingen (2010). Metrics include the coefficient of determination (R^2) and the root-mean-square-error (RMSE).

Table 3
Summary of SPA-Crop at-harvest cumulative sum (i.e. from sowing to harvest) of SPA-Crop flux estimates (Mod.) compared to EC-derived data (EC) for GPP, R_{eco} and NEE for crop growing seasons from 2006 to 2015. Metrics include the percentage observed–modelled differences (Δ).

	GPP (gC per m^{-2})			R_{eco} (gC per m^{-2})			NEE (gC per m^{-2})		
Crop type (season)	Obs. GPP	Mod. GPP	Δ (%)	Obs. Reco	Mod. Reco	Δ (%)	Obs. NEE	Mod. NEE	Δ (%)
Wheat (2006/2007)	1214	1080	−11	917	785	−14	−305	−306	0
Wheat (2008/2009)	1089	1141	5	757	609	−20	−342	−544	59
Wheat (2010/2011)	1323	1209	−9	845	885	5	−491	−334	−32
Wheat (2013/2014)	1265	1334	5	799	916	15	−467	−426	−9
Barley (2004/2005)	943	1109	18	680	700	3	−282	−412	46
Barley (2011/2012)	1352	1418	5	936	857	−8	−462	−581	26
Barley (2014/2015)	1087	1291	19	752	803	7	−383	−507	32
Rapeseed (2007/2008)	1185	975	−18	1024	642	−37	−219	−358	64
Rapeseed (2012/2013)	1045	1006	−4	672	629	−6	−391	−381	−3
Pea (2010)	24	23	−5	247	231	−6	−52	−48	−7
Average	1053	1058	1	763	706	−6	−339	−390	18

Table 4
At-harvest yield values (g C m^{-2}) – a comparison between observed yield (Obs.) and SPA-Crop model estimates (Mod.). Metrics include the percentage observed–modelled differences (Δ).

Crop type (season)	Obs. Yield	Mod. Yield	Δ (%)
Wheat (2006/2007)	255	244	−4
Wheat (2008/2009)	239	247	3
Wheat (2010/2011)	272	238	−13
Wheat (2013/2014)	258	255	−1
Barley (2004/2005)	287	242	−16
Barley (2011/2012)	322	252	−22
Barley (2014/2015)	300	236	−21
Rapeseed (2007/2008)	182	173	−5
Rapeseed (2012/2013)	152	237	56
Pea (2010)	30	43	43

4.2. SPA-Crop cumulative fluxes and yields

SPA-Crop generally overestimated the cumulative NEE when compared with the EC measurements. However, the measured-modelled differences varied on a per season basis and did not reveal any crop-specific biases. This inter-seasonal variability in cumulative NEE indicates uncertainty related to the simulated respiration as opposed to the crop-specific parameters determining photosynthesis and development (see table in the online supplementary information). In spite of this, given the high spatiotemporal resolution of the model, this research demonstrates that SPA-Crop could be a powerful tool for investigating the impacts of variable environmental drivers (e.g. radiation and temperature). Furthermore, although this evaluation was based on a comparison to NEE, if the model was combined with additional post-harvest management information that would result in intra- or inter-annual changes to soil C stocks (e.g. tillage and residual management), SPA-Crop could be used for simulating the influence of different management scenarios on the long-term net biome production of the Oensingen crop rotation (Emmel et al., 2018).

The SPA-Crop yield estimates shows that the model does provide a resonable simulation of C allocation to the storage organ – particularly for wheat and barley. The modelled yields for the wheat seasons were comparable to results detailed in Hastings et al. (2010) who estimated yield with a bias of +5% using the denitrification de-composition (DNDC) model for simulating an Oensingen wheat season (2003/2004). However, the two models have different approaches towards yield simulation: SPA-Crop yield estimates are based on daily photoperiod and temperature, whereas DNDC has a user-defined maximum potential yield that is reduced by water and nitrogen stresses. In the original SPA-Crop development, Sus et al. (2010) reported large biases in yield estimates of −17% and −36% for the Oensingen 2006/2007 wheat and 2004/2005 barley seasons, respectively. By comparison, in this research, seasons we demonstrate a clear reduction in these negative yield biases for both seasons with the yield being underestimated by −4% and −16% for the 2006/2007 wheat and 2004/2005 barley seasons, respectively. We are, therefore, confident that the parameter updates applied here improved the yield simulation for winter wheat and winter barley. In particular, while Sus et al. (2010) sourced values from literature, we updated parameters related to leaf area and nitrogen distribution at specific layer heights based on field measurements (see online supplementary information). These parameter changes have influenced both the canopy structure, which determines the intercepted

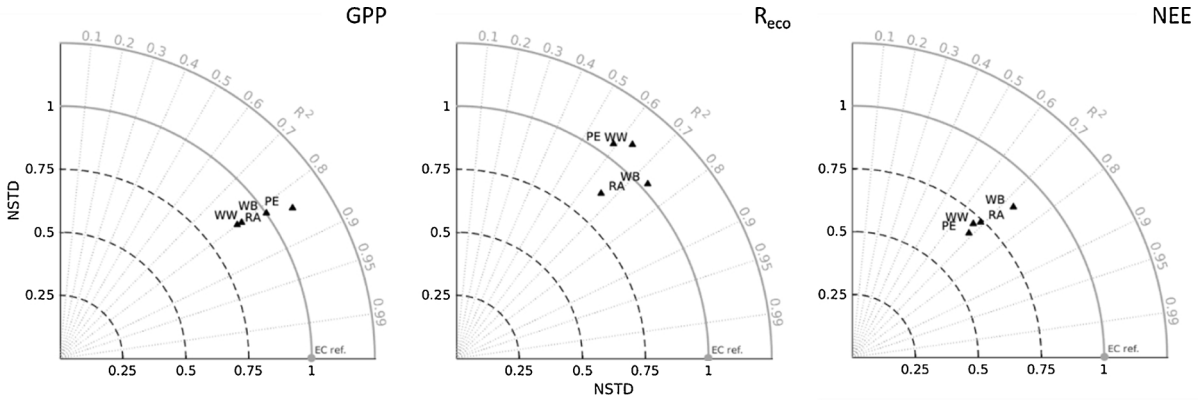

Fig. 5. Normalised Taylor diagrams summarising the SPA-Crop model performance of GPP (left), R_{eco} (middle) and NEE (right) simulations for each crop type (black triangles): winter wheat (WW), winter barley (WB), rapeseed (RA) and pea (PE). The plots are within a polar coordinate system where the coefficient of determination (R^2) is included on the polar angle and the normalised standard deviation (NSTD) is shown along the polar axes (radial dashed lines). The grey 1:1 line and dot (EC ref.) represent the corresponding EC-derived data used as a reference.

solar radiation, and the leaf-scale photosynthetic capacity, resulting in a more superior representation of for wheat crops.

4.3. Model deficiencies and recommendations for further development

The seasonality of the daily SPA-Crop GPP estimates closely matched the EC fluxes, however, some systematic differences in magnitude were observed. These differences were observed for the simulated peak GPP for winter wheat and rapeseed, which were underestimated by an average of -4.7 and -6.8 gC m^{-2} d^{-1} for winter wheat and rapeseed, respectively. The timing of the peak CO_2 assimilation is largely determined by crop phenology (i.e. developmental stage), whereas the magnitude of GPP estimates is controlled by the SPA-Crop photosynthesis parameters (Sus et al., 2010), which are fixed throughout the crop seasons. Thus, it would be expected that further research involving refining these parameters, particularly those related to the carboxylation rate (V_{cmax} and J_{max}), will increase the simulated maximum GPP for wheat and rapeseed.

For each crop season, the cumulative and daily simulation of R_{eco}, and subsequently NEE, had a relatively weaker agreement with the EC fluxes than that of GPP. Since NEE is measured directly using the EC approach, whereas GPP is derived from NEE using a partitioning model, we deduce that both the partitioning model and the SPA-Crop model appear to demonstrate a similar photosynthetic assimilation. However, larger discrepancies exist between the two models with regards to the R_{eco}. Across the growing seasons, the R^2 values for R_{eco} and NEE were also more variable ($0.61 \leq R^2 \leq 0.85$). Although, this variability in R_{eco} could be due to errors in the simulation of both the autotrophic and heterotrophic respiration, the fraction of autotrophic respiration was set differently for each crop type. Yet, this SPA-Crop/EC data misfit appears to be independent of crop type, suggesting that the model handles autotrophic respiration consistently. On the other hand, SPA-Crop simulates heterotrophic respiration as the sum of respiration from the litter and SOC pools, which are calculated according to the soil C content and the mineralisation rate. Consequently, uncertainty can exist in both the initial C content prescribed to the SPA-Crop litter C and SOC pools and the mineralisation rate that was assigned to each of the two components. Most notably for the winter wheat and barley sesons, this uncertainty in the litter and SOC pools is further confirmed by a consistently negative bias in the R_{eco} simulation over the winter months. During this period the photosynthesis of the winter crops would be minimal and so the heterotrophic response of soil would dominate the EC data. As a consequence of the R_{eco} being underestimated during these early development stages, the cumulative NEE was frequently overestimated.

The SPA-Crop initial C contents assigned to the litter and SOC pools were estimated based on sampling carried out on dates near the beginning of the study period in Autumn 2005. For additional crop growing seasons, estimates of the initial litter C were derived based on the manure application and crop harvest residues recorded in the Oensingen management history. However, soil tillage was not accounted for, which would have led to a decline in SOC prior to the sowing of successive crop seasons (Mishra et al., 2010; Xue et al., 2015). The management information did also not consider the remaining below-ground biomass (i.e. root litter). However, if we assume a harvest index of 0.4, 0.5, 0.3 and 0.4 for wheat, barley, rapeseed and pea crops respectively (Fan et al., 2017), and an average ratio of above to below ground crop residue of 0.22 (IPCC, 2006), then we estimate that only a relatively small amount of C would remain in the soil – between 86 gC m^{-2} (wheat) and 19 gC m^{-2} (rapeseed), based on the average yield for each crop type. Since estimates of initial SOC were fixed according to the initial empirical measurements, we concede that the long-term crop management at Oensingen would have resulted in a net loss in soil C (Emmel et al., 2018) and, thus, our initial estimates are likely to be too high. Research done by Hastings et al. (2010), involving the DNDC model soil parameters, demonstrated that uncertainty in initial SOC produced large uncertainties in soil respiration.

The heterotrophic respiration does depend on the amount of C in the litter and SOC pools, however, so too is the decomposability of this C for soil microorganisms and, thus, microbial respiration (Schmidt et al., 2011; Cotrufo et al., 2013). SPA-Crop uses a fixed mineralisation rate set for the two pools. However, in reality this rate would vary depending on the carbon-to-nitrogen (C:N) ratio (Nicolardot et al., 2001). Since the model only considers leaf nitrogen per area, thus does not simulate the above- or below-ground nitrogen cycle, C:N ratio measurements of soil and litter would be useful to understand how easily the available C of harvest residues is consumed by microbes. Specifically, soil C:N measurements throughout the crop-rotation could be used to constrain the mineralisation rate in SPA-Crop.

We observed a particularly large difference in R_{eco} between the SPA-Crop and EC data at the beginning of the 2006/2007 wheat growing season. A likely explanation of this disagreement is due to a previously failed potato crop season. The potatoes were sown on 3rd May 2006; however, the crop was damaged by a hailstorm on 6th July 2006. Although, some secondary growth did occur, the quality of the resulting tubers was considered insufficient for harvest, and the vegetation was subsequently ploughed under on 18th October 2006 in preparation for the wheat season. Since the potato crop was not harvested and the biomass remained in the field, the litter C and SOC content at the time of sowing the wheat was most likely exceptionally high, which would have enhanced heterotrophic respiration. Thus, the absence of available soil C analysis data, particularly around the beginning of the 2006/2007 wheat season, meant that SPA-Crop could not resolve this relatively labile C for heterotrophic respiration.

Crop yield estimates generally matched observations, however, the yield was overestimated for most seasons. Although, nitrate-based fertilisers were applied throughout the growing season to support photosynthetic CO_2 assimilation, the yield formation simulated by SPA-Crop could still have been unrealistically optimum.This overestimate could be attributed to the model not simulating the impacts of nitrogen stress.

The yield estimates for the simulated 2012/2013 rapeseed season overestimated the observations by +56%, however, the daily and cumulative GPP estimates for this season had a high agreement with EC data. Conversely, for the 2007/2008 rapeseed season, the modelled GPP had a negative bias, whereas the yield had only a relatively small measured-modelled difference of −5%. This model performance in the yield estimates for the two seasons suggests an issue with the C allocation to the storage organ of the rapeseed crops. For rapeseed, we used C allocation fractions from Penning de Vries et al. (1989). However, we recommend further laboratory analysis of the C allocation to the root, stem, foliage and storage organs in a similar manner to that carried out for the pea crop season. With regards to the discrepancies in GPP, this can be attributed to the early emergence of the 2007/2008 crop. Because of this early development, the 2007/2008 season reached the end of the vegetative period at the beginning of May already, when conditions for photosynthesis – temperature and photoperiod – were less favourable than during the 2012/2013 season, when the same developmental stage was reached approximately one month later. An approach to address this early development and effectively delay emergence would be to apply a calibration to the cardinal temperatures – minimum, maximum and optimum – required for the vernalisation of winter rapeseed.

During the 13 year-analysis period, most of the crop growing seasons was either winter wheat or barley (Table 1). Thus, the empirical basis for the SPA-Crop evaluation was much better for the winter cereal crops when compared to that of rapeseed and pea. Additional rapeseed and pea crop growing seasons would therefore be beneficial for the improvement of SPA-Crop. However, the Proof of Ecological Performance rules determining crop rotation at the Oensingen site require a minimum 3-year break between consecutive rapeseed crops, whereas a 6-year break is required between two pea crops. Such crop rotations consequently limit the analysis of additional pea seasons and, thus,

highlight the requirement for roving tower flux measurements on nearby fields.

5. Conclusions

Using long-term observations recorded at the Oensingen cropland site, we have demonstrated that SPA-Crop daily C flux estimates have a resonable agreement with EC fluxes. The model can simulate the general timings and magnitudes of net CO_2 exchange determining the cropland C balance for wheat, barley, rapeseed and pea crops (NEE had a mean $R^2 = 0.70$; mean RMSE = 1.3 gC m^{-2} d^{-1}). With regards to the at-harvest budgets, the mean cumulative NEE had a measured-modelled difference of +15% per crop season, while the mean yield was overestimated by +2%. We conclude that this high model performance is due to model calibration, including critical crop-specific measurements made at the field site, which allowed for a realistic simulation of crop development and photosynthesis.

A novelty of our research included a SPA-Crop parameterisation for simulating the growth of pea crops. Based on the agreement between the pea SPA-Crop NEE to that of the EC measurements ($R^2 = 0.69$; RMSE = 0.9 g C m^{-2} d^{-1}) for a single growing season, we have shown that this model calibration provides reasonable results. For all crop growing seasons, we suggest that a more realistic simulation of heterotrophic respiration, and thus R_{eco} and NEE, could be achieved by including more information related to the litter C and SOC pools. We also recommend refinements to the model's photosynthesis-related parameters – particularly around the period of peak GPP for wheat and rapeseed. Given the success of the model for the simulation of winter crops and peas, we have demonstrated that SPA-Crop provides a reliable simulation of C fluxes and yields across crop types used in European agriculture.

Acknowledgements

This research was supported by the Swiss National Science Foundation, grant 200021_146373. AR undertook the model simulations and data comparisons with support, including the provision of flux and biometric data, from all other authors. We acknowledge the use of meteorological data from Agroscope Reckenholz, Zürich, provided by Christof Ammann and are grateful for the collaboration and detailed farm management information received from the farmers Walter and Daniel Ingold.

References

Abi Saab, M.T., Todorovic, M., Albrizio, R., 2015. Comparing AquaCrop and CropSyst models in simulating barley growth and yield under different water and nitrogen regimes. Does calibration year influence the performance of crop growth models? Agric. Water Manag. 147, 21–33.

Abdalla, M., Osborne, B., Lanigan, G., Forristal, D., Williams, M., Smith, P., Jones, M.B., 2013. Conservation tillage systems: a review of its consequences for greenhouse gas emissions. Soil Use Manage. 29, 199–209.

Alaoui, A., Goetz, B., 2008. Dye tracer and infiltration experiments to investigate macropore flow. Geoderma 144, 279–286.

Angulo, C., Rötter, R., Lock, R., Enders, A., Fronzek, S., Ewert, F., 2013. Implication of crop model calibration strategies for assessing regional impacts of climate change in Europe. Agric. For. Meteorol. 170, 32–46.

Baldocchi, D., Falge, E., Gu, L., Olson, R., Hollinger, D., Running, S., Anthoni, P., Bernhofer, C., Davis, K., Evans, R., Fuentes, J., Goldstein, A., Katul, G., Law, B., Lee, X., Malhi, Y., Meyers, T., Munger, W., Oechel, W., Paw, K.T., Pilegaard, K., Schmid, H.P., Valentini, R., Verma, S., Vesala, T., Wilson, K., Wofsy, S., 2001. FLUXNET: a new tool to study the temporal and spatial variability of ecosystem scale carbon dioxide, water vapor, and energy flux densities. Bull. Am. Meteorol. Soc. 82, 2415–2434.

Begcy, K., Walia, H., 2015. Drought stress delays endosperm development and misregulates genes associated with cytoskeleton organization and grain quality proteins in developing wheat seeds. Plant Sci. 240, 109–119.

Boote, K.J., Jones, J.W., White, J.W., Asseng, S., Lizaso, J.I., 2013. Putting mechanisms into crop production models. Plant Cell Environ. 36, 1658–1672.

Buyanovsky, G.A., Wagner, G.H., 1987. Carbon transfer in a winter wheat (Triticum aestivum) ecosystem. Biol. Fertil. Soils 5, 76–82.

Ceschia, E., Béziat, P., Dejoux, J.F., Aubinet, M., Bernhofer, C., Bodson, B., Buchmann, N., Carrara, A., Cellier, P., Di Tommasi, P., Elbers, J.A., Eugster, W., Grünwald, T., Jacobs, C.M.J., Jans, W.W.P., Jones, M., Kutsch, W., Lanigan, G., Magliulo, E., Marloie, O., Moors, E.J., Moureaux, C., Olioso, A., Osborne, B., Sanz, M.J., Saunders, M., Smith, P., Soegaard, H., Wattenbach, M., 2010. Management effects on net ecosystem carbon and GHG budgets at European crop sites. Agric. Ecosyst. Environ. 139, 363–383.

Challinor, A.J., Watson, J., Lobell, D.B., Howden, S.M., Smith, D.R., Chhetri, N., 2014. A meta-analysis of crop yield under climate change and adaptation. Nat. Clim Change advance online publication.

Cotrufo, M.F., Wallenstein, M.D., Boot, C.M., Denef, K., Paul, E., 2013. The Microbial Efficiency-Matrix Stabilization (MEMS) framework integrates plant litter decomposition with soil organic matter stabilization: do labile plant inputs form stable soil organic matter? Glob. Chang. Biol. 19, 988–995.

The Swiss Federal Council, 2015. Ordinance on Organic Farming and the Labelling of Organically Produced Products and Foodstuffs (Organic Farming Ordinance) of 22 September 1997 (as of 1 January 2015) (Swiss Council Regulation no. 910.18). pp. 40.

Cowan, I.R., 1978. Stomatal behaviour and environment. In: Preston, R.D., Woolhouse, H.W. (Eds.), Advances in Botanical Research. Academic Press, pp. 117–228.

Deryng, D., Sacks, W.J., Barford, C.C., Ramankutty, N., 2011. Simulating the effects of climate and agricultural management practices on global crop yield. Glob. Biogeochem. Cycles 25, GB2006.

Dietiker, D., Buchmann, N., Eugster, W., 2010. Testing the ability of the DNDC model to predict CO2 and water vapour fluxes of a Swiss cropland site. Agric. Ecosyst. Environ. 139, 396–401.

Emmel, C., Winkler, A., Hörtnagl, L., Revill, A., Ammann, C., D'Odorico, P., Buchmann, N., Eugster, W., 2018. Integrated management of a Swiss cropland is not sufficient to preserve its soil carbon pool in the long-term. Biogeosci. Discuss. 2018, 1–29.

Eugster, W., Moffat, A.M., Ceschia, E., Aubinet, M., Ammann, C., Osborne, B., Davis, P.A., Smith, P., Jacobs, C., Moors, E., Le Dantec, V., Béziat, P., Saunders, M., Jans, W., Grünwald, T., Rebmann, C., Kutsch, W.L., Czerný, R., Janouš, D., Moureaux, C., Dufranne, D., Carrara, A., Magliulo, V., Di Tommasi, P., Olesen, J.E., Schelde, K., Olioso, A., Bernhofer, C., Cellier, P., Larmanou, E., Loubet, B., Wattenbach, M., Marloie, O., Sanz, M.-J., Søgaard, H., Buchmann, N., 2010. Management effects on European cropland respiration. Agric. Ecosyst. Environ. 139, 346–362.

Ewert, F., Rötter, R.P., Bindi, M., Webber, H., Trnka, M., Kersebaum, K.C., Olesen, J.E., van Ittersum, M.K., Janssen, S., Rivington, M., Semenov, M.A., Wallach, D., Porter, J.R., Stewart, D., Verhagen, J., Gaiser, T., Palosuo, T., Tao, F., Nendel, C., Roggero, P.P., Bartošová, L., Asseng, S., 2015. Crop modelling for integrated assessment of risk to food production from climate change. Environ. Model. Softw. 72, 287–303.

Fan, J., McConkey, B., Janzen, H., Townley-Smith, L., Wang, H., 2017. Harvest index–yield relationship for estimating crop residue in cold continental climates. Field Crops Res. 204, 153–157.

Farquhar, G.D., von Caemmerer, S., 1982. Modelling of photosynthetic response to environmental conditions. In: Lange, O.L., Nobel, P.S., Osmond, C.B., Ziegler, H. (Eds.), Physiological Plant Ecology II. Springer, Berlin Heidelberg, pp. 549–587.

Gabaldón-Leal, C., Webber, H., Otegui, M.E., Slafer, G.A., Ordóñez, R.A., Gaiser, T., Lorite, I.J., Ruiz-Ramos, M., Ewert, F., 2016. Modelling the impact of heat stress on maize yield formation. Field Crops Res. 198, 226–237.

Hansen, J.W., 2002. Realizing the potential benefits of climate prediction to agriculture: issues, approaches, challenges. Agric. Syst. 74, 309–330.

Hastings, A.F., Wattenbach, M., Eugster, W., Li, C., Buchmann, N., Smith, P., 2010. Uncertainty propagation in soil greenhouse gas emission models: An experiment using the DNDC model and at the Oensingen cropland site. Agric. Ecosyst. Environ. 136, 97–110.

Hillel, D., 1980. Fundamentals of Soil Physics. Academic Press.

Huang, Y., Yu, Y., Zhang, W., Sun, W., Liu, S., Jiang, J., Wu, J., Yu, W., Wang, Y., Yang, Z., 2009. Agro-C: A biogeophysical model for simulating the carbon budget of agroecosystems. Agric. For. Meteorol. 149, 106–129.

IPCC, 2006. 2006 IPCC guidelines for national greenhouse gas inventories. In: Eggleston, H.S., B.L, Miwa, K., Ngara, T., Tanabe, K. (Eds.), Intergovernmental Panel on Climate Change (IPCC).

Jones, H.G., 2013. Plants and Microclimate: A Quantitative Approach to Environmental Plant Physiology. Cambridge University Press, Cambridge.

Kärnä, T., Baptista, A.M., 2016. Evaluation of a long-term hindcast simulation for the Columbia River estuary. Ocean Model. (Oxf) 99, 1–14.

Kollas, C., Kersebaum, K.C., Nendel, C., Manevski, K., Müller, C., Palosuo, T., Armas-Herrera, C.M., Beaudoin, N., Bindi, M., Charfeddine, M., Conradt, T., Constantin, J., Eitzinger, J., Ewert, F., Ferrise, R., Gaiser, T., Cortazar-Atauri, I.Gd., Giglio, L., Hlavinka, P., Hoffmann, H., Hoffmann, M.P., Launay, M., Manderscheid, R., Mary, B., Mirschel, W., Moriondo, M., Olesen, J.E., Öztürk, I., Pacholski, A., Ripoche-Wachter, D., Roggero, P.P., Roncossek, S., Rötter, R.P., Ruget, F., Sharif, B., Trnka, M., Ventrella, D., Waha, K., Wegehenkel, M., Weigel, H.-J., Wu, L., 2015. Crop rotation modelling—A European model intercomparison. Eur. J. Agron. 70, 98–111.

Lehuger, S., Gabrielle, B., Cellier, P., Loubet, B., Roche, R., Bäziat, P., Ceschia, E., Wattenbach, M., 2010. Predicting the net carbon exchanges of crop rotations in Europe with an agro-ecosystem model. Agric. Ecosyst. Environ. 139, 384–395.

Lloyd, J., Taylor, J.A., 1994. On the temperature dependence of soil respiration. Funct. Ecol. 8, 315–323.

Matthews, R.B., Rivington, M., Muhammed, S., Newton, A.C., Hallett, P.D., 2013. Adapting crops and cropping systems to future climates to ensure food security: the role of crop modelling. Glob. Food Sec. 2, 24–28.

Mercado, L.M., Bellouin, N., Sitch, S., Boucher, O., Huntingford, C., Wild, M., Cox, P.M., 2009. Impact of changes in diffuse radiation on the global land carbon sink. Nature 458, 1014–1017.

Mishra, U., Ussiri, D.A.N., Lal, R., 2010. Tillage effects on soil organic carbon storage and

dynamics in Corn Belt of Ohio USA. Soil Tillage Res. 107, 88–96.
Moureaux, C., Debacq, A., Hoyaux, J., Suleau, M., Tourneur, D., Vancutsem, F., Bodson, B., Aubinet, M., 2008. Carbon balance assessment of a Belgian winter wheat crop (Triticum aestivum L.). Glob. Chang. Biol. 14, 1353–1366.
Moureaux, C., Ceschia, E., Arriga, N., Béziat, P., Eugster, W., Kutsch, W.L., Pattey, E., 2012. Eddy covariance measurements over crops. In: Aubinet, M., Vesala, T., Papale, D. (Eds.), Eddy Covariance: A Practical Guide to Measurement and Data Analysis. Springer, Netherlands, Dordrecht, pp. 319–331.
Nicolardot, B., Recous, S., Mary, B., 2001. Simulation of C and N mineralisation during crop residue decomposition: a simple dynamic model based on the C:N ratio of the residues. Plant Soil 228, 83–103.
Parkes, B., Defrance, D., Sultan, B., Ciais, P., Wang, X., 2018. Projected changes in crop yield mean and variability over West Africa in a world 1.5 K warmer than the pre-industrial era. Earth Syst. Dyn. Discuss. 9, 119–134.
Penning de Vries, F.W.T., Jansen, D.M., ten Berge, H.F.M., Bakema, A.H., 1989. Simulation of Ecophysiological Processes in Several Annual Crops. Simulation Monographs. Pudoc, Wageningen, Netherlands.
Porter, Semenov, M.A., 2005. Crop responses to climatic variation. Philos. Trans. R. Soc. B Biol. Sci. 360, 14.
Rawls, J.W., Brakensiek, L.D., Saxton, E.K., 1982. Estimation of Soil Water Properties.
Reichstein, M., Falge, E., Baldocchi, D., Papale, D., Aubinet, M., Berbigier, P., Bernhofer, C., Buchmann, N., Gilmanov, T., Granier, A., Grünwald, T., Havránková, K., Ilvesniemi, H., Janous, D., Knohl, A., Laurila, T., Lohila, A., Loustau, D., Matteucci, G., Meyers, T., Miglietta, F., Ourcival, J.-M., Pumpanen, J., Rambal, S., Rotenberg, E., Sanz, M., Tenhunen, J., Seufert, G., Vaccari, F., Vesala, T., Yakir, D., Valentini, R., 2005. On the separation of net ecosystem exchange into assimilation and ecosystem respiration: review and improved algorithm. Glob. Chang. Biol. 11, 1424–1439.
Reichstein, M., Bahn, M., Ciais, P., Frank, D., Mahecha, M.D., Seneviratne, S.I., Zscheischler, J., Beer, C., Buchmann, N., Frank, D.C., Papale, D., Rammig, A., Smith, P., Thonicke, K., van der Velde, M., Vicca, S., Walz, A., Wattenbach, M., 2013. Climate extremes and the carbon cycle. Nature 500, 287–295.
Revill, A., Sus, O., Barrett, B., Williams, M., 2013. Carbon cycling of European croplands: a framework for the assimilation of optical and microwave Earth observation data. Remote Sens. Environ. 137, 84–93.
Richards, L.A., 1931. Capillary conduction of liquids through porous mediums. Physics 1, 318–333.
Rogiers, N., Eugster, W., Furger, M., Siegwolf, R., 2005. Effect of land management on ecosystem carbon fluxes at a subalpine grassland site in the Swiss Alps. Theor. Appl. Climatol. 80, 187–203.
Rötter, R.P., Palosuo, T., Kersebaum, K.C., Angulo, C., Bindi, M., Ewert, F., Ferrise, R., Hlavinka, P., Moriondo, M., Nendel, C., Olesen, J.E., Patil, R.H., Ruget, F., Takáč, J., Trnka, M., 2012. Simulation of spring barley yield in different climatic zones of Northern and Central Europe: a comparison of nine crop models. Field Crops Res. 133, 23–36.
Saxton, K.E., Rawls, W.J., Romberger, J.S., Papendick, R.I., 1986. Estimating generalized soil-water characteristics from texture. Soil Sci. Soc. Am. J. 50, 1031–1036.
Schmidt, M.W.I., Torn, M.S., Abiven, S., Dittmar, T., Guggenberger, G., Janssens, I.A., Kleber, M., Kögel-Knabner, I., Lehmann, J., Manning, D.A.C., Nannipieri, P., Rasse, D.P., Weiner, S., Trumbore, S.E., 2011. Persistence of soil organic matter as an ecosystem property. Nature 478, 49.
Smith, P., Lanigan, G., Kutsch, W.L., Buchmann, N., Eugster, W., Aubinet, M., Ceschia, E., Béziat, P., Yeluripati, J.B., Osborne, B., Moors, E.J., Brut, A., Wattenbach, M., Saunders, M., Jones, M., 2010. Measurements necessary for assessing the net ecosystem carbon budget of croplands. Agric. Ecosyst. Environ. 139, 302–315.
Streck, N., Weiss, A., Xue, Q., Stephen Baenziger, P., 2003. Improving predictions of developmental stages in winter wheat: a modified Wang and Engel model. Agric. For. Meteorol. 115, 139–150.
Sus, O., Williams, M., Bernhofer, C., Beziat, P., Buchmann, N., Ceschia, E., Doherty, R., Eugster, W., Grunwald, T., Kutsch, W., Smith, P., Wattenbach, M., 2010. A linked carbon cycle and crop developmental model: description and evaluation against measurements of carbon fluxes and carbon stocks at several European agricultural sites. Agric. Ecosyst. Environ. 139, 402–418.
Taylor, K.E., 2001. Summarizing multiple aspects of model performance in a single diagram. J. Geophys. Res. Atmos. 106, 7183–7192.
Therond, O., Hengsdijk, H., Casellas, E., Wallach, D., Adam, M., Belhouchette, H., Oomen, R., Russell, G., Ewert, F., Bergez, J.-E., Janssen, S., Wery, J., Van Ittersum, M.K., 2011. Using a cropping system model at regional scale: low-data approaches for crop management information and model calibration. Agric. Ecosyst. Environ. 142, 85–94.
Valade, A., Vuichard, N., Ciais, P., Ruget, F., Viovy, N., Gabrielle, B., Huth, N., Martiné, J.-F., 2013. ORCHIDEE-STICS, a process-based model of sugarcane biomass production: calibration of model parameters governing phenology. GCB Bioenergy n/a-n/a.
Vuichard, N., Ciais, P., Viovy, N., Li, L., Ceschia, E., Wattenbach, M., Bernhofer, C., Emmel, C., Grünwald, T., Jans, W., Loubet, B., Wu, X., 2016. Simulating the net ecosystem CO2 exchange and its components over winter wheat cultivation sites across a large climate gradient in Europe using the ORCHIDEE-STICS generic model. Agric. Ecosyst. Environ. 226, 1–17.
Wattenbach, M., Sus, O., Vuichard, N., Lehuger, S., Gottschalk, P., Li, L., Leip, A., Williams, M., Tomelleri, E., Kutsch, W.L., Buchmann, N., Eugster, W., Dietiker, D., Aubinet, M., Ceschia, E., Baziat, P., Granwald, T., Hastings, A., Osborne, B., Ciais, P., Cellier, P., Smith, P., 2010. The carbon balance of European croplands: a cross-site comparison of simulation models. Agric. Ecosyst. Environ. 139, 419–453.
Webber, H., Gaiser, T., Ewert, F., 2014. What role can crop models play in supporting climate change adaptation decisions to enhance food security in Sub-Saharan Africa? Agric. Syst. 127, 161–177.
White, J.W., Hoogenboom, G., Kimball, B.A., Wall, G.W., 2011. Methodologies for simulating impacts of climate change on crop production. Field Crops Res. 124, 357–368.
Williams, M., Rastetter, E.B., Fernandes, D.N., Goulden, M.L., Wofsy, S.C., Shaver, G.R., Melillo, J.M., Munger, J.W., Fan, S.M., Nadelhoffer, K.J., 1996. Modelling the soil-plant-atmosphere continuum in a Quercus–Acer stand at Harvard Forest: the regulation of stomatal conductance by light, nitrogen and soil/plant hydraulic properties. Plant Cell Environ. 19, 911–927.
Williams, M., Law, B.E., Anthoni, P.M., Unsworth, M.H., 2001. Use of a simulation model and ecosystem flux data to examine carbon-water interactions in Ponderosa Pine. Tree Physiol. 21, 287–298.
Xue, J.-F., Pu, C., Liu, S.-L., Chen, Z.-D., Chen, F., Xiao, X.-P., Lal, R., Zhang, H.-L., 2015. Effects of tillage systems on soil organic carbon and total nitrogen in a double paddy cropping system in Southern China. Soil Tillage Res. 153, 161–168.
Yu, S., Eder, B., Dennis, R., Chu, S.-H., Schwartz, S.E., 2006. New unbiased symmetric metrics for evaluation of air quality models. Atmos. Sci. Lett. 7, 26–34.
Zhang, W., Ricketts, T.H., Kremen, C., Carney, K., Swinton, S.M., 2007. Ecosystem services and dis-services to agriculture. Ecol. Econ. 64, 253–260.
Zheng, H., Li, Y., Chen, J.M., Wang, T., Huang, Q., Huang, W.X., Li, S.M., Yuan, W.P., Zheng, X., Zhang, S.P., Chen, Z.Q., Jiang, F., 2014. A global carbon assimilation system based on a dual optimization method. Biogeosci. Discuss. 11, 14269–14317.